FINAL REPORT

A Comprehensive Analysis of Electron Conical Distributions From Multi-Satellite Databases

Principal Investigator: J. Douglas Menietti
Department of Physics & Astronomy, University of Iowa, Iowa City, IA 52242
(NASA Project No. NAG5-2102; U of I Project No. 14251600)

Overview

This report consists of a copy of a paper that has been submitted to the Journal of Geophysical Research, entitled "DE 1 and Viking Observations Associated With Electron Conical Distributions," and an abstract of another paper (included as an appendix to the report) that is about to be submitted to the same journal entitled "Perpendicular Electron Heating by Absorption of Auroral Kilometric Radiation." A bibliography of other papers that have been published as a result of this project follows.

The purpose of this project was to use the DE 1 and Viking particle and wave data to better understand the source mechanism of electron conical distributions. We have shown that electron conics are often associated with upper hybrid waves in the nightside auroral region. We have also shown that electron conics are observed near auroral kilometric radiation (AKR) source regions and may be the result of perpendicular heating due to waves [Menietti et al., 1993a, 1993b, 1993c]. We have completed a statistical study of electron conics observed by DE-1 and Viking. The study shows the occurrence frequency and location of electron conical distributions [Menietti et al., 1993c]; there are some differences between the results of DE and Viking perhaps due to different regions sampled.

In the first paper of this report we show that electron conics may also be associated with regions of parallel oscillating electric fields as observed on DE-1. This corroborates the work of Andre and Eliasson [1992], and indicates that electron conics may have multiple generation sources. We also show examples of "90-degree" electron conics and suggest they may magnetically fold to appear at higher altitudes as "ordinary" electron conics.

In the second paper (the abstract is included as an appendix), we investigate the role of AKR in heating electrons perpendicular to the magnetic field (thus producing "90-degree" electron conics). We show that the damping rate for AKR in a warm electron plasma is high enough to suggest that the electrons are perpendicularly heated. We also solve the diffusion equation for a Maxwellian plasma in the presence of AKR, and we compare model contour plots of the phase-space distribution function to the DE-1 observations in AKR near-source regions.

Other Papers Published Papers as a Result of this Project:

Menietti, J. D., C. S. Lin, H. K. Wong, A. Bahnsen, and D. A. Gurnett, Association of electron conical distributions with upper hybrid waves, J. Geophys. Res., 97, 1353, 1992.

Menietti, J. D., J. L. Burch, R. M. Winglee, and D. A. Gurnett, DE 1 particle and wave observations in auroral kilometric radiation (AKR) source regions, J. Geophys. Res., 98, 5865, 1993a.

Menietti, J. D. and J. L. Burch, DE-1 Particle and wave observations in an AKR source region, Auroral Plasma Dynamics, AGU Monograph 80, ed. by R. L. Lysak, American Geophysical Union, Washington, D.C., p. 239, 1993b.

Menietti, J. D., Observations of electron conical distributions and possible productions mechanisms, to appear in Physics of Space Plasmas (1992), Proceedings of the 1992 Cambridge Workshop in Theoretical Geoplasma Physics held in August, 1992, in press, 1993c.

References

Andre, M. and L. Eliasson, Electron acceleration by low frequency electric field fluctuations: electron conics, Geophys. Res. Lett., 19, 1073, 1992.

Wong, H. K. and M. L. Goldstein, A mechanism for bursty radio emission in planetary magnetospheres, Geophys. Res. Lett., 17, 2229, 1990.

The following paper has been submitted to Journal of Geophysics Research:

DE 1 and Viking Observations Associated with Electron Conical Distributions

J. D. Menietti[1], D. R. Weimer[2], M. Andre[3] and L. Eliasson[4]
[1]Department of Physics and Astronomy, University of Iowa, Iowa City, Iowa 52242
[2]Geophysical Institute, University of Alaska, Fairbanks, AK 99775
[3]Swedish Institute of Space Physics, University of Umea, S-901 87 Umea, Sweden
[4]Swedish Institute of Space Physics, POB 812, S-981 28 Kiruna, Sweden

Abstract

Data from the electron detectors on board the Swedish Viking satellite launched during a period of low solar activity, and from the DE 1 satellite launched during active solar conditions, have been examined for the occurrence and location of electron conical distributions and several conclusions can be drawn. First, we note that most of the best examples of electron conics observed by the V-3 experiment onboard Viking occurred in the afternoon sector in the range of magnetic local time 14 hrs < MLT < 18 hrs, at mid-altitudes in the range 10,000 km

$< h <$ 13,500 km, with few occurring in the nightside auroral region, a region poorly sampled at altitudes greater than 5000 km . For the Viking data, there is no correlation of electron conics with upper hybrid waves. DE 1 observations made by the high altitude plasma instrument (HAPI) indicate that electron conics were observed in the mid-morning sector and the late evening sector, and as has been reported earlier, the correlation with upper hybrid waves was good. The HAPI did not sample the afternoon sector. The electron conics observed on both satellites occurred in the presence of at least a modest (several kV) potential difference beneath the satellite with a maximum energy that was usually, but not always, equal to or greater than the maximum energy of the electron conics.

Two independent sets of observations by DE 1 suggest two distinct production mechanisms for electron conics. Examination of DE 1 electric field measurements from the plasma wave instrument (PWI) during the observation of electron conics show simultaneous parallel oscillations in the frequency range 0.2 Hz $< f <$ 0.5 Hz during one and perhaps two of four events examined, and upper hybrid waves were observed on all four events. In addition, recent observations of "90-degree" electron conics associated with AKR source regions suggest a perpendicular heating mechanism produced by wave-particle interaction. Such distributions may be observed as electron conics at higher altitudes. These results suggest more than one possible source mechanism may be responsible for electron conics observed by DE 1.

I. Introduction

Many papers have recently appeared discussing the generation mechanisms for electron conical distributions since their discovery in the DE 1 data set by Menietti and Burch [1985]. The latter authors, who observed the electron conics (ec's) associated with trapped particles and parallel electric fields, suggested a wave-particle interaction and perpendicular heating as a source mechanism, in analogy with ion conic formation. Lundin et al. [1987] and Hultqvist et al. [1988] have reported observations of electron conics in the Viking data and suggested that a parallel potential that varied in magnitude over a fraction of an electron bounce period might explain electron conics that were observed associated with ion conics. At present the outstanding question being addressed by investigators is "Is the dominant generation mechanism of electron conics due to perpendicular (oblique) or parallel heating/acceleration processes?"

Wong et al. [1988] have shown that upper hybrid waves generated by an electron distribution with $\partial f/\partial v_\perp > 0$ can heat the electrons oblique to the magnetic field. Subsequently, numerical simulations of the production of electron conics by local (mid-altitude) upper hybrid waves using a loss cone [Roth et al., 1990] and a loss cone with a ring distribution (Lin et al., 1990; Menietti et al., 1990) have shown the effectiveness of the mechanism. The parameters used for these studies were for distributions present in the nightside auroral region at mid-altitudes. Beghin et al. [1989] performed an extensive study of narrow-banded, higher frequency emissions using data from the AUREOL/ARCAD 3 satellite at high latitude and at altitudes between 400 and 2000 km. They found no upper hybrid frequency emissions. In addition, Benson [1991] has shown from a comprehensive analysis of ISIS 1 and ISIS 2 data that upper hybrid waves occur on low-altitude orbits of the auroral region on only about 1% of the passes. However, at higher altitudes the observations differ. Farrell et al. [1990] have reported numerous examples of narrowband wave intensifications at frequencies between 1.1 to

1.3 times the local gyrofrequency in the mid-altitude polar cusp region. Menietti et al. [1992] have shown using both DE 1 and Viking data that intense upper hybrid waves exist in the mid-altitude region and, for the case of the DE 1 data, these waves are often associated with electron conics at mid-altitudes of the nightside and dayside auroral regions.

Roth et al. [1990] and Temerin and Cravens [1990] (extending the ideas of Lundin et al. [1987]) have demonstrated that an electron conical distribution can result from parallel heating of the electrons via electrostatic or acoustic mode waves. Upon mirroring, this heated electron distribution resembles electron conical distributions. Subsequently, Temerin and Cravens [1990] have demonstrated with a test particle simulation of the electron distribution that electron-conic-like distributions can be produced purely by stochastic acceleration of the electrons parallel to a dipole magnetic field. They suggested that Alfven-ion cyclotron waves, known to be associated with inverted-V electron precipitation may produce the parallel acceleration. Lysak [1991] has shown that ULF Alfven waves in the frequency range 0.1 Hz to 1 Hz are expected from realistic models of the "Alfven resonator" along auroral field lines, where electron conics are observed.

Electron conics observed to date are all associated with parallel potentials and upward ion beams or ion conics. Andre and Eliasson [1992, 1993] have shown that the electron conic energy and the ion beam energy are correlated in the Viking data, indicating a possible relationship between the potential beneath the satellite and the formation of the electron conic. These authors have subsequently shown by simulation that low-frequency oscillations of the parallel electric field (with a period of roughly 1 Hz) are sufficient to generate electron conical distributions. They chose plasma parameters consistent with those measured both by Viking and DE 1. In this model the electrons are in resonance with a fluctuating $E_{\parallel}$. Importantly, Andre and Eliasson find that the model is not extremely sensitive to the frequency of the oscillations. They tested their model with a sample of broadband waves in the frequency range of $0.1 < f < 30$ Hz and found they could generate "electron conic" signatures. Andre and Eliasson also point out that low-frequency oscillations of $E_{\parallel}$ have been observed in the Viking data [Block and Falthammar, 1990].

To understand this mechanism, we note that the travel time for an auroral electron from the acceleration region at an altitude of several thousand kilometers via magnetic mirroring above the ionosphere and back to the acceleration region, is about 1 second. Thus, several electrons may be accelerated by one $E_{\parallel}$ on their way down, and then slowed down by a smaller $E_{\parallel}$ on their way up, in this way gaining energy. This mechanism is attractive, e.g., since large amounts of energy are associated with the parallel electric field and since variations of electric fields on auroral field lines at roughly 1 Hz often are observed.

Andre and Eliasson [1992, 1993] also compared electron energization in the parallel direction at high altitude with perpendicular heating at low altitude, and found virtually identical "electron conic" signatures at high or mid-altitudes. Andre and Eliasson [1993] discuss oblique and perpendicular heating at mid-altitudes. They find that perpendicular or oblique diffusion in a limited region (14500 km to 16500 km geocentric distance) produces "electron conics" with a distinct "V-shape," similar to many ion conics, and different from most observed electron conics which show flux peaks just outside the loss cone. They point out that Viking does not observe upper hybrid waves associated with electron conics, thus they believe oscillations of $E_{\parallel}$ are the prime candidate for the production of electron conics.

In this paper we present a limited statistical study of electron conics observed by both DE 1 and Viking. We will show some of the similarities and the differences in the observations of electron conical distributions, and attempt to reconcile these observations with current models for generation mechanisms. We present new electric field measurements from the plasma wave instrument (PWI) on board DE 1 that indicate that, at least on one of four possible examples of electron conics, there may be substantial oscillations of $E_{\parallel}$ at a frequency near 0.5 Hz, in agreement with the model of Andre and Eliasson [1992]. In addition, DE 1 data suggest that intense waves near AKR source centers may provide substantial electron heating perpendicular to the magnetic field.

II. Observations of Electron Conics

A. Characteristic Signature

There have been a number of distributions appearing in the literature that have been referred to as "electron conics." Electron conics are generally considered distributions of electrons that have maxima in the pitch angle range $130° \leq \alpha \leq 180°$ just outside of the loss cone. Typically the electron conic distribution is the most energetic, but in some cases it may appear as the most intense flux, such as the example shown in Plate 2 of Menietti and Burch [1985]. On energy-versus-time spectrograms the signature is parallel stripes centered on a pitch angle of 180° such as shown for the pass of day 309 of 1981 shown in Plate 1 of Menietti and Burch [1985]. In Figure 1 we display a contour plot of the distribution function obtained during one spin (6 sec) of the DE 1 satellite during a pass on day 81/289; this plot clearly shows the signature of the electron conic with enhanced flux lying just outside the loss cone. In a later section we will present observations of what might be termed "90-degree" electron conics, i.e. electron distributions lying in a pitch angle range centered around 90°. We would, however, distinguish electron conics from "bi-directional distributions" as discussed by Burch et al. [1990]. Burch et al. have determined that electron distributions resembling "bi-directional conics" are expected when the satellite is within a region of parallel electric fields. These distributions of electrons are distinguished by their bi-directional character with upgoing and downgoing electrons having the same energy (see Figures 1 and 2 of Burch et al. [1990]) and are distinct from electron conics as discussed in this paper.

B. Statistical Survey of Viking and DE 1 Data

Electron data from the V-3 experiment (Rickard Lundin, PI) were examined for orbits 1 to over 1200. This data exists on microfiche as color spectrograms of energy-versus-time with energy flux color-coded. The resolution allowed a relatively easy identification of electron conics. There were a number of low intensity, isolated examples or examples showing non-characteristic signatures which were not included in our statistics. We summarize what are considered good examples of electron conics observed in the Viking and DE 1 data in Tables 1 and 2, respectively. By "good" examples we mean clear signatures that persist for multiple spins of the satellite.

Table 1

Viking Observations of Electron Conics

Orbit	Range of times (UT) (hr, min)	Range of invariant latitude	Range of MLT (hrs)	Range of altitude (km)	UH waves present
168	1023 - 1026	79.7° - 79.4°	13.1 - 13.1	11476 - 11716	no
343	0529 - 0539	78.1° - 79.2°	14.2 - 13.0	11021 - 11855	?
392	0259 - 0308	75.3° - 78.2°	16.4 - 15.2	9741 - 10734	no
452	0045 - 0047	78.3° - 78.9°	16.3 - 16.1	10467 - 10674	no
524	0311 - 0314	78.1° - 78.6°	13.1 - 12.5	12552 - 12717	no
552	0517 - 0522	75.0° - 76.2°	14.0 - 13.4	12467 - 12746	no
626	1548 - 1551	72.3° - 73.6°	16.1 - 16.1	11615 - 11846	no
658	1143 - 1144	74.5° - 74.8°	15.3 - 15.3	12970 - 13013	no
730	1351 - 1354	76.7° - 77.7°	15.1 - 15.1	13276 - 13356	no
736	1554 - 1559	76.8° - 78.7°	14.5 - 14.5	13015 - 13205	no

Table 2

DE 1 Observations of Electron Conics

year-day	Range of times (UT) (hr, min)	Range of invariant latitudes	Range of MLT (hrs)	Range of altitude (km)	UH waves present
81261	0752 - 0753	69.6° - 70.0°	22.1 - 21.4	13772 - 13917	yes
81261	2147 - 2151	62.4° - 60.6°	23.7 - 23.6	11713 - 10995	yes
81281	0732 - 0733	63.6° - 63.1°	21.18 - 21.2	10496 - 10670	yes
81278	1349 - 1352	77.3° - 77.9°	10.22 - 10.21	18696 - 19004	yes
81279	1047 - 1050	78.3° - 78.8°	11.46 - 11.52	20836 - 21045	yes
81309	0635 - 0638	67.4° - 65.7°	19.23 - 19.31	10290 - 10839	yes
81289	2044 - 2047	70.9° - 70.0°	22.34 - 22.27	13080 - 12500	yes

Tables 1 and 2 show some interesting statistics. First, the number of examples of electron conics is not very large, only ten good examples from Viking and fewer from DE 1. Albeit, there are many other isolated and weaker examples, in each data set. There were also a number of examples from the DE 1 data set for which wave data was not available. In both data sets the electron conics were always observed associated with field-aligned potentials with upflowing ions accelerated beneath the satellite, indicating the presence of an upward-directed electric field. As observed by Viking, the maximum energy of the ion beams is equal to or larger than the energy of the electron conics. This is almost always the case for the DE 1 data, but there were several exceptions, for example the pass of day 81/279 in Table 2. The ec's observed by Viking were not associated with upper hybrid waves, while those observed by DE 1 were.

While the range of invariant latitude for each satellite is similar, the local time sectors do not overlap. The best observations of ec's by Viking are in the mid-afternoon sector. It is important to note, however, that coverage of the local time sector, 20−24 MLT by Viking occurred almost exclusively for altitudes less than 5000 km. This may be the reason that no electron conics were observed by Viking in the nightside auroral region. We also mention that isolated examples of clear electron conics (one spin only) did occur in the evening sector, such as for orbit 418 at an altitude of 9999 km, invariant latitude of 79.4°, and a magnetic local time of 18.24 hours. The DE 1 high altitude plasma instrument did not sample the mid-afternoon sector in 1981, but found good examples of ec's in the nightside auroral region as well as some in the dayside auroral region. It may be that the ec signatures observed by each satellite have a different source mechanism unique to the location of the observation. It should also be noted that the DE 1 observations were made during a period of solar maximum while the Viking data were obtained during solar minimum.

III. Electric Field Oscillations Associated With Electron Conics

A. Data Analysis

The measurement of low frequency electric field oscillations may be accomplished with the plasma wave instrument (PWI) on DE 1. The characteristics of this instrument are described in detail by Shawhan et al. [1981]. Oscillations at a frequency around 1 Hz are below the range of the conventional plasma wave receivers, but they can be detected by using a special processing of the quasi-static electric field data. With this processing it is also possible to determine if the electric field oscillations are predominately parallel or perpendicular to the ambient magnetic field.

The quasi-static electric field in the DE 1 spin/orbit plane is obtained with a long-wire "double probe," measuring 200 m tip-to-tip. This antenna is perpendicular to the satellite spin axis, which in turn is approximately perpendicular to the geomagnetic field in the polar magnetosphere. The electric field data are digitally sampled at a frequency of 16 Hz, which establishes an upper frequency limit at the 8 Hz Nyquist frequency. As the satellite spins with a six-second period, the quasi-static electric field data are modulated with a 1/6 Hz sine wave. In other words, electric field fluctuations at frequencies below the spin rate are transformed to

a 1/6 Hz signal. The "static" electric fields, and the fluctuations up to 1/12 Hz, are normally determined by a measurement of the amplitude and phase of this 1/6 Hz signal. The detection of oscillations at frequencies above the spin rate and below 8 Hz requires a different processing technique.

The usual method to determine the frequency power spectra of the electric field would be to use either a discrete Fourier transform of the digital data, or a Maximum Entropy Method analysis. These techniques will not work in this case, due to the rotation of the double-probe antenna. To show why, we use a simple illustrative example. Shown in Figure 2a is a hypothetical 1 Hz electric field oscillation, perpendicular to the ambient magnetic field. The amplitude as a function of time is drawn with a dash-dot-dashed line. For reference, the sine of the angle between the rotating antenna and the magnetic field is shown with the dotted line. The magnetic field lines are assumed to lie in the spin plane. The electric field signal that would be measured with the rotating antenna is determined by multiplying the original signal by the sine function, resulting in the signal that is shown with the solid line. It is important to note that during every 3 sec half-spin this measured signal is exactly 180° out of phase with the signal during the other half-spin.

A Fourier transform of this measured signal would fail to detect the original 1 Hz oscillation due to the alternating phase shifts. Instead, two false peaks would be detected at beat frequencies of $1 \pm 1/6$ Hz. In order to correct this problem with the phase shift we multiply the measured signal by the sine of the rotation angle between the antenna and the ambient magnetic field. The result is shown as the solid line in Figure 2b. As this processed signal now has a coherent phase the peak at 1 Hz can be detected by normal spectral analysis techniques. At this point the original wave signal has now been multiplied by a sine-squared function, so that the peak amplitude is equal to the (constant) amplitude of the wave.

In order to correct for the phase reversals that are introduced by the antenna rotation, it was assumed that the wave oscillation was perpendicular to the magnetic field. If the oscillation were parallel to the magnetic field we would need to multiply by the cosine of the phase angle, rather than the sine of the angle, in order to achieve the proper phase correction. We can use this fact to determine whether or not an unknown, measured signal is due to oscillations that are predominately parallel or perpendicular to the magnetic field. To show how, we complete our example illustration with Figure 2c, which shows the result of multiplying the measured signal by the cosine function. The result has complicated phase shifts and the amplitude is not as large as that which was obtained with the sine multiplication. A spectral analysis of this signal would not produce a significant peak at 1 Hz.

The situation would be reversed if the hypothetical wave had a parallel rather than perpendicular orientation. In this case the spectral peak would show up in the signal that was processed through multiplication by the cosine function rather than the sine function.

To summarize, the measured electric field signal, which has had phase reversals introduced by the rotating antenna, is multiplied by the sine of the rotation angle between the antenna and the magnetic field. We call this the "perpendicular" signal. The measured time series is also multiplied with the cosine of the angle to produce a separate "parallel" signal. These two separate time series are then processed to determine the frequency power spectrum. A strong peak in the "perpendicular" signal that is not present in the "parallel" signal is

indicative of an electric field oscillation that is orientated predominately perpendicular to the magnetic field, and vice versa.

Random noise will have nearly equal strength in the perpendicular and parallel signals, and will show up as a particularly strong peak at the spin frequency and higher harmonics, due to our phase multiplication. Best results are also obtained if the strong spin-modulated "DC" signal is first removed with a 1/6 Hz band-rejection digital filter before the phase multiplication step.

For the actual power spectrum analysis of this data we still find that a Fourier transform gives unsatisfactory results, due to aliasing and leakage between frequencies. It is often difficult to determine which peaks are real and which are artifacts of the FFT. We prefer to use a set of digital band-pass filters, as described in any textbook on digital signal processing. The data are simply passed through the multiple filters, and the outputs are squared and summed over any desired integration period. To normalize, the sums from each filter are divided by the number of data points times the filters' bandwidth, to obtain the conventional power spectrum units of $(mV/m)^2/Hz$. For the results to be shown here, we have used an integration period of 12 sec with 44 separate filters that are equally spaced on a logarithmic scale between 1/6 and 8 Hz. For convenience, each filter has a band-pass frequency that is $2^{1/8}$ times the frequency of the previous filter, so that a frequency doubling is obtained at every eighth step. The optimal band-width for each filter in this case is about 0.09 times the pass frequency.

B. Results of E-Field Analysis

To apply this technique we selected four passes that contained some of the best examples of electron conics. For two of these passes only spin modulation of the signals was obtained, with no detectable presence of significant oscillations of the electric field at low frequencies. For the passes of days 81/289 and possibly 81/309, parallel oscillations of E are present.

In Figures 3 and 4 we display plots of the spectral analysis technique applied to the passes of days 81/289 and 81/309, respectively. Each figure shows relative amplitude of the electric field intensity parallel to the magnetic field, $E_{\parallel}$, versus frequency (Hz) for six times during each pass. Each plot represents a period of 12 seconds of processed data during a time when excellent examples of electron conics were present in the particle data. The vertical dotted lines indicate the location of multiples of the spin frequency which is 0.165 Hz. Peaks at or very near these times must be considered due to spin modulation and artifacts of the data processing. The arrows on each plot indicate significant peaks that do not seem to be associated with spin modulation harmonics. Some of the panels have peaks between 0.2 and 0.5 Hz that may represent significant oscillations of $E_{\parallel}$ at the time. For several of the panels the peaks observed in Figure 3 for 81/289 at a frequency of approximately 0.4 Hz are significant; the peaks observed in Figure 4 near $f \sim 0.3$ Hz are weaker and close to a satellite spin harmonic. For 81/289 the electron conics were observed at an altitude of about 13,000 km and the potential beneath the satellite as indicated by the highest energy of the upward ion beams is between 10 kV and 20 kV. We estimate the magnitude of the electric field oscillations for this pass are in the range of 10 mV/m $< E <$ 20 mV/m (cf. Figure 5a), but $E_{\parallel}$ is in the range of $2.4 < E_y < 6$ mV/m with an average of about 3.9 mV/m based on the power spectral densities in Figure 3. For the pass of day 81/309 the parameters are similar; the altitude of the spacecraft at the time of the observations was also

in the range 10 kV < E < 20 kV. The magnitude of the electric field oscillations is estimated to be in the range of 5 mV/m <E < 10 mV/m (cf. Figure 5b) with $E_{\parallel} \approx 1.7$ mV/m (Figure 3).

C. Model of $E_{\parallel}$

Using the model of parallel oscillations of the electric field [Andre and Eliasson, 1992] we have attempted to reproduce the electron conics observed on the pass of 81/289. We refer the reader to the reference for details of the model. A time-varying electric field is assumed to exist along the magnetic field in the range r = 16,400 km to 18,400 km (the satellite geocentric distance was 19,400 km). An absorbing atmosphere is assumed at a distance of r = 6500 km, and the magnetic field is assumed to be dipolar. The form of the electric field is

$$E_{\parallel} = E_s + E_t, \qquad (1)$$

where $E_s = 7.5$ mV/m is the static field and $E_t = 2$ mV/m is the time-varying part, thus, the total static potential in the model is 15 kV. The frequency of oscillation is assumed to be spread over a small bandwidth from 0.3 Hz < f < 0.6 Hz (according to the procedure described in Andre and Eliasson [1992]). Downgoing electrons are injected at the upper boundary of the potential drop by randomly selecting 5×10^4 particles from a 1.1 keV Maxwellian distribution. The particle start times were spread out over 6.66 seconds, which is twice the lowest wave frequency. The electrons are then followed numerically in small time steps until they are either lost in the atmosphere or reach r = 19,400 km again. The result is displayed in Figure 6a, a plot of contours of the model distribution function, which clearly represents an electron conical distribution similar to that shown in Figure 1. The parameters chosen are not exactly those measured, but are similar. In particular, the oscillating field, E_s, is probably smaller than observed. During the time period shown in Figure 6b, we estimate from Figure 3 that $E_{\parallel} \approx$ 2.4 mV/m. One problem is that the large potential beneath the satellite has the effect of producing an upward distribution with too large a temperature compared to the observations. In Figure 6b we have superimposed the contours of the distribution function obtained from the data (solid lines) with those of the model (shaded contours). The agreement is quite good. The ratio of the temperature of the upward to downward flowing electrons for the distribution shown in Figure 6a is $T\uparrow/T\downarrow = 1.36$, which is quite close to the observed value of ~ 1.3. Using the average energy of the observed distribution, we similarly find $E\uparrow/E\downarrow = 1.16$. If the magnitude of E_s is increased, the distribution becomes more extended along $V_{\parallel}$, and the ratio of $T\uparrow/T\downarrow$ becomes larger. We suggest reasons for these discrepancies in the discussion below.

IV. Electron Heating Associated with Akr Source Centers

Temerin and Cravens [1990] suggested that auroral kilometric radiation might heat electrons perpendicular to the magnetic field. We have investigated several cases of possible electron heating associated with near-AKR source region crossings of the DE 1 spacecraft (cf. Menietti et al. [1993]). During the lifetime of the high altitude plasma instrument, DE 1 intercepted the nightside auroral region at altitudes in the range of ~ 8000 km to ~ 13000 km. The AKR source region is believed to be located usually in the altitude range 3000 to 8000 km. (cf. Roux et al. [1993]). Menietti et al. [1993] present particle and wave data obtained by DE 1 during several near-source crossings of AKR at unusually high altitudes. Plate 2 of the latter paper displays the electron and AC magnetometer data for the nightside auroral region pass of

day 285 of 1981 at an altitude of about 11500 km. Just equatorward of the region when DE 1 is believed to be closest to the source center is a region where the electron distribution has a strong temperature anisotropy, with $T_\perp/T_\parallel >> 1$. In Figure 7 we display a contour of the distribution function taken in that region. This is likely to be an example of perpendicular heating of the electrons due to wave-particle interactions and the resulting distribution may be referred to as a "90-degree" electron conic. While flowing upward such distributions will fold to smaller pitch angles due to conservation of the first adiabatic invariant. At higher altitude such a distribution may look more like the distribution shown in Figure 1. If such "90-degree" conics are produced near to an AKR source at typical altitudes of about 5000 km, then "folded" electron conics (such as Figure 1) would be observed at altitudes of about 10,000 km (DE 1 altitudes in the nightside auroral region during 1981.) A cartoon scenario of this process is depicted in Figure 8.

One argument against this hypothesis is that examples of electron conics at intermediate pitch angles (such as are observed for ion conics) have not been observed. Electron conics are observed either just outside the loss cone or near 90°. No systematic search for intermediate pitch angles has been conducted, however, and only a few passes near the AKR source region are available for DE 1. Also, good examples of electron conic distributions are themselves somewhat rare.

V. Summary

In this paper we have briefly reviewed observations of electron conical distributions and discussed some of the attempts at modelling these phenomena. The models to date have emphasized either parallel or oblique heating of the plasma. The parallel heating may be due to oscillations of the DC field-aligned potential as modelled by Andre and Eliasson [1992], or stochastic heating due to, for example, Alfven ion-cyclotron waves [Temerin and Cravens, 1990]. Alternatively, the oblique heating may be due to upper hybrid waves and/or possibly perpendicular heating due to AKR emissions (cf. Figure 7). Figure 9 is a plot of the power spectral density of the AC electric field obtained by the plasma wave instrument on board DE 1. This data was obtained during the time that electron conics were observed on the pass of day 81/289. Upper hybrid waves (electrostatic peak indicated) were present during this pass as well as parallel oscillations of the electric field and may have produced oblique heating of the electrons as suggested by Wong et al. [1988].

We summarize the observations of Viking and DE 1 as follows: The Viking data indicate a strong correlation of electron conics with field-aligned potentials as evidenced by the presence of upward ion beams beneath the satellite. The data also indicate that the maximum energy of the electron conics is always less than or equal to the maximum energy of the ion beams. This is consistent with the model of resonance of electrons with low-frequency fluctuations of $E_\parallel$. While some of the Viking examples of electron conics are associated with low-frequency oscillations of the parallel electric field, there are no cases which are associated with upper hybrid waves. The Viking observations of the best examples of electron conics were made almost exclusively in the afternoon sector of local time, but this may be solely a result of almost no coverage of the evening sector ($20 < MLT < 24$) at altitudes greater than 5000 km.

The DE 1 observations also show a strong correlation of electron conics with the presence of field-aligned potential, and usually, but not always, the maximum energy of the electron conic is less than or equal to the maximum energy of the upward ion beams seen simultaneously. The electron conics are observed both in the nightside and the dayside auroral region, but no data was obtained for the mid-morning sector. The DE 1 data indicate an association of upper hybrid waves with the presence of electron conics. Recent observations indicate that strong temperature anisotropies with $T_\perp/T_\parallel >> 1$ are observed associated with AKR source regions. These distributions may be considered "90-degree" electron conics, and would magnetically fold to appear at higher altitudes more like the electron conic shown in Figure 1. Initial examination of electric field data on DE 1 indicates that on one and perhaps two of four passes examined, low-frequency fluctuations of $E_\parallel$ in the frequency range 0.2 Hz $< f <$ 0.5 Hz occur coincident with "good" examples of electron conics observed. Parameters close to those observed on one of these events are used to model an electron conic produced by oscillations of $E_\parallel$. The simulated electron conic is a reasonable reproduction of those observed indicating the feasibleness of the concept.

VI. Discussion

At the present time it is not possible to definitively determine a dominant production mechanism of electron conics. As indicated above, there are arguments and observations that support either a parallel or oblique heating mechanism. Models of both mechanisms agree with the data to date. It is perhaps informative to consider the possibility that both types of mechanisms operate. This view may be supported by the fact that the Viking observations of ec's which show no correlation with upper hybrid waves, are seen in the mid-afternoon sector. In contrast, the DE 1 observations are observed in the day and nightside auroral regions and do show some correlation with upper hybrid waves. Upper hybrid waves are observed simultaneously with oscillations of $E_\parallel$ for the pass of 81/289 presented here. In fact, based on the DE 1 observations discussed above, some nightside auroral region electron conics may have been produced as "90-degree" ec's at lower altitudes near the AKR source region.

A more definitive test of these theories will be to determine if low-frequency fluctuations of $E_\parallel$ occur simultaneously with the electron conics, as we have attempted in this study. While a high correlation of ec's with wave activity may not be found due to the large growth rate for candidate waves, this may not be the case for oscillations of $E_\parallel$. Somewhere along the field line, oscillations of $E_\parallel$ must be taking place simultaneously (in time but not necessarily in space) with the observation of electron conics in order for the resonance phenomena to occur. Two of the four passes studied in section III contained good examples of electron conics but no parallel oscillations of the electric field were observed. This may be due to oscillations of $E_\parallel$ along the field line but not at the satellite altitude. At least one of the four passes, however, is a good candidate for oscillations of $E_\parallel$. It may be important to note that the two cases (of the four examined) which did not show oscillations of $E_\parallel$ both occurred in the dayside auroral region. We point out that the region of parallel potential in the model is 1000 km beneath the satellite even though observations of oscillating $E_\parallel$ were obtained simultaneously with the electron conics. It was necessary to locate the region of oscillating $E_\parallel$ away from the satellite in order to avoid electron distributions that were extended along $V_\parallel$. The fact that the simulation

of the electron conic required parameters that did not exactly match the observations (see section III) can be explained in a number of ways:

1) the potential structure was different from that assumed;
2) the oscillating potential has a temporally varying magnitude;
3) the spectrum of oscillation frequencies was different from that used in the model; or
4) oblique heating of the distribution contributed to the formation of the ec.

While it is possible to investigate each of these modifications to the model, such a study is beyond the scope of this present work, the purpose of which is to show the feasibility of the concept of oscillations of $E_\parallel$ rather than a detailed model.

Other useful observations which would allow a more definitive (but not sufficient) statement to be made about the dominant production mechanism of ec's are the following:

1) Observations of ec's on a field line with no observable parallel electric field any where along the magnetic field line;
2) Ion beam energies much less than simultaneous ec energies; or
3) Observations of $n_\uparrow/n_\downarrow > 1$ for a specific $v_\parallel$ within an ec.

Observations 1 and 2 would not be totally consistent with production of the ec by an oscillating $E_\parallel$. For (1), we note that as we pointed out above, oscillations of $E_\parallel$ could be occurring at a different altitude; thus, a simultaneous (multi-satellite) measurement of $E_\parallel$ at various altitudes along the field line would be necessary. For (2), if we assume that $E_t \leq E_s/2$ in Equation 1, then in the oscillating $E_\parallel$ model, the energy of the ec is at most the potential of the electric field beneath the satellite. In item 3, n is the number density of upward or downward electrons. Number 3 is not consistent with stochastic heating parallel to B for large distances along the field line [cf. Temerin and Cravens, 1990], but is still consistent with the oscillating $E_\parallel$ model. We note, however, that in the model of oscillating $E_\parallel$ parallel presented here (Figure 6), $n_\uparrow \approx 0.8\ n_\downarrow$. This may be a result of the short altitude range over which the oscillating potential was allowed to operate.

High resolution observations of both particles and fields are necessary to resolve these issues. Multiprobe satellites would be excellent for these studies, and we eagerly await the results of the Swedish Freja satellite which is able to resolve both the electron conics as well as low frequency fluctuations of the electric field.

Acknowledgements

JDM gratefully acknowledges the assistance of T. Potemra and L. Zanetti for making the Viking particle data available. Special thanks to Michelle Govostes and Kathy Kurth for clerical assistance and to Joyce Chrisinger for drafting some of the figures. This work was supported at Iowa by NASA grant NAG5-1552 and at Alaska by NASA grant NAG5-2249.

References

Andre, M. and L. Eliasson, Electron acceleration by low frequency electric field fluctuations: Electron conics, *Geophys. Res. Lett.*, *19*, 1073, 1992.

Andre, M. and L. Eliasson, Some electron conic generation mechanisms, *Proceedings of AGU Chapman Conference on Micro- and Mesoscale Phenomena in Space Plasmas held in Kauai*, HI, in press, 1993.

Beghin, C. and J. L. Rauch, and J. M. Bosqued, Electrostatic plasma waves and HF auroral hiss generated at low altitude, *J. Geophys. Res.*, *94*, 1359, 1989.

Benson, R. A., Elusive upper hybrid waves in the auroral topside ionosphere, abstract for Chapman Conference on Auroral Plasma Dynamics, Minneapolis, MN, October 21-25, 1991.

Block, L. P. and C. G. Falthammar, The role of magnetic-field-aligned electric fields in auroral acceleration, *J. Geophys. Res.*, *95*, 5877, 1990.

Burch, J. L., C. Gurgiolo, and J. D. Menietti, The electron signature of parallel electric fields, *Geophys. Res. Lett.*, *17*, 2329, 1990.

Farrell, W. M., D. A. Gurnett, J. D. Menietti, H. K. Wong, C. S. Lin, J. L. Burch, Wave intensifications near the electron cyclotron frequency within the polar cusp, *J. Geophys. Res.*, *95*, 6493, 1990.

Hultqvist, B., R. Lundin, K. Stasiewicz, L. Block, P.-A. Lindqvist, G. Gustafsson, H. Koskinen, A. Bahnsen, T. A. Potemra, and L. J. Zanetti, Simultaneous observation of upward moving field aligned energetic electrons and ions on auroral zone field lines, *J. Geophys. Res.*, *93*, 9765, 1988.

Lin, C. S., J. D. Menietti, and H. K. Wong, Perpendicular heating of electrons by upper hybrid waves generated by a ring distribution, *J. Geophys. Res.*, *95*, 12295, 1990.

Lundin, R., L. Eliasson, B. Hultqvist, and K. Stasiewicz, Plasma energization on auroral field lines as observed by the Viking satellite, *Geophys. Res. Lett.*, *14*, 443, 1987.

Lysak, R. L., Feedback instability of the ionospheric resonant cavity, *J. Geophys. Res.*, *96*, 1553, 1991.

Menietti, J. D., and J. L. Burch, Electron conic signatures observed in the nightside auroral zone and over the polar cap, *J. Geophys. Res.*, *90*, 5345, 1985.

Menietti, J. D., C. S. Lin, and H. K. Wong, The correlation of ring distributions with electron conics: Simulations of the production of upper hybrid waves, *Physics of Space Plasmas (1989)*, *9*, 455, 1990.

Menietti, J. D., C. S. Lin, H. K. Wong, A. Bahnsen, and D. A. Gurnett, Association of electron conical distributions with upper hybrid waves, *J. Geophys. Res.*, *97*, 1353, 1992.

Menietti, J. D., J. L. Burch, R. M. Winglee, and D. A. Gurnett, DE-1 particle and wave observations in AKR source regions, *J. Geophys. Res.*, *98*, 5865, 1993.

Roth, I., M. K. Hudson, and M. Temerin, Generation models of electron conics, *J. Geophys. Res.*, *94*, 10095, 1990.

Roux, A. et al., Auroral kilometric radiation sources: In situ and remote observations from Viking, *J. Geophys. Res.*, *98*, 11657, 1993.

Shawhan, S. D., D. A. Gurnett, D. A. Odem, R. A. Helliwell, and C. G. Park, The plasma wave and quasi-static electric field instrument (PWI) for Dynamics Explorer-A, *Space Sci. Instrum.*, *5*, 535-550, 1981.

Temerin. M. A. and D. Cravens, Production of electron conics by stochastic acceleration parallel to the magnetic field, *J. Geophys. Res.*, *95*, 4285, 1990.

Wong, H. K., J. D. Menietti, C. S. Lin, and J. L. Burch, Generation of Electron Conical Distributions by Upper Hybrid Waves in the Earth's Polar Region, *J. Geophys. Res.*, *93*, 10025, 1988.

Figure Captions

Figure 1. Contours of the distribution function in $v_{\parallel}$-$v_{\perp}$ space for a one-spin (6 sec.) period of a nightside auroral region pass of day 289, 1981. The times are indicated on the plot. Positive $v_{\parallel}$ is along the magnetic field (toward Earth). The electron conics are seen as enhancements of the distribution function just outside the loss cone. The dots are the data points.

Figure 2a A hypothetical 1 Hz electric field oscillation, perpendicular to the ambient magnetic field. The amplitude as a function of time is drawn with a dash-dot-dashed line. For reference, the sine of the angle between the rotating antenna and the magnetic field is shown with the dotted line.

Figure 2b. The same as Figure 2a but now the measured signal is multiplied by the sine of the antenna angle an displayed as the solid line. This represents the electric field parallel to the magnetic field.

Figure 2c. The result of multiplying the measured signal by the cosine function to generate the signal perpendicular to the magnetic field.

Figure 3. Relative amplitude of the electric field intensity parallel to the magnetic field, $E_{\parallel}$, versus frequency (Hz) for three consecutive times during the pass of 81/289. Each panel represents a period of 12 seconds of processed data during a time when electron conics were present in the particle data.

Figure 4. Same as Figure 3, but for the pass of day 81/309.

Figure 5. Measured total electric field amplitude in the spin-plan versus time for the pass of day 81/289 (Figure 5a) and for the pass of day 81/309 (Figure 5b).

Figure 6a. Contours of the electron distribution function for the model electron conic for parameters similar to those for the pass of day 81/289. For this simulation parallel oscillations of the electric field were assumed at a frequency of $f = 0.45$ Hz.

Figure 6b. Contours of the model electron conic (shaded) superimposed on contours of the observed distribution function (solid lines).

Figure 7. Contours of the distribution function for a period during the nightside auroral region pass. The format is the same as Figure 1. This data was taken just equatorward of a near-AKR source region and shows a strong temperature anisotropy, with $T_{\perp}/T_{\parallel} > 1$. This can be defined as a "90-degree" (pitch angle) electron conic.

Figure 8. A cartoon of the hypothetical scheme for generating "folded" electron conics at mid-altitude nightside auroral regions from "90-degree" electron conics produced adjacent to AKR source centers at lower altitude.

Figure 9. Power spectral density versus frequency obtained by PWI during observations of electron conics on the pass of day 81/289. Note the presence of upper hybrid

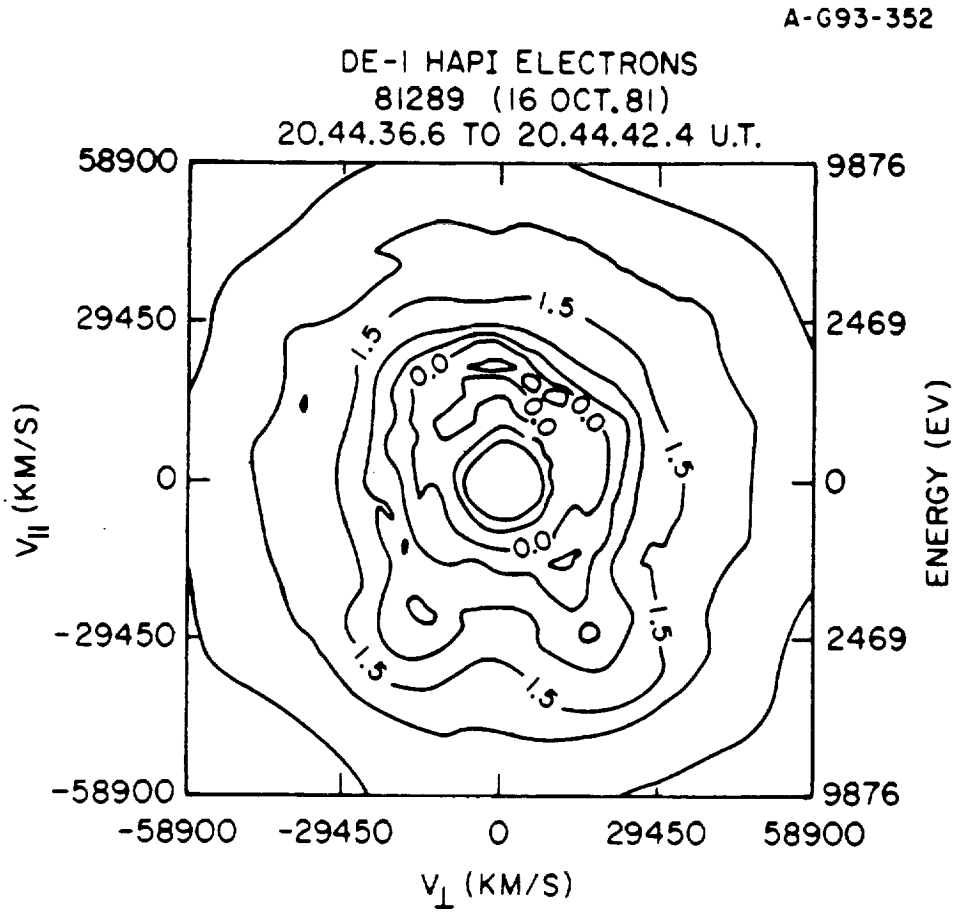
A-G93-352
DE-1 HAPI ELECTRONS
81289 (16 OCT. 81)
20.44.36.6 TO 20.44.42.4 U.T.
58900
29450
0
-29450
-58900
9876
2469
0
2469
9876
1.5
0.0
$V_{||}$ (KM/S)
ENERGY (EV)
-58900
-29450
0
29450
58900
$V_{\perp}$ (KM/S)

Figure 1

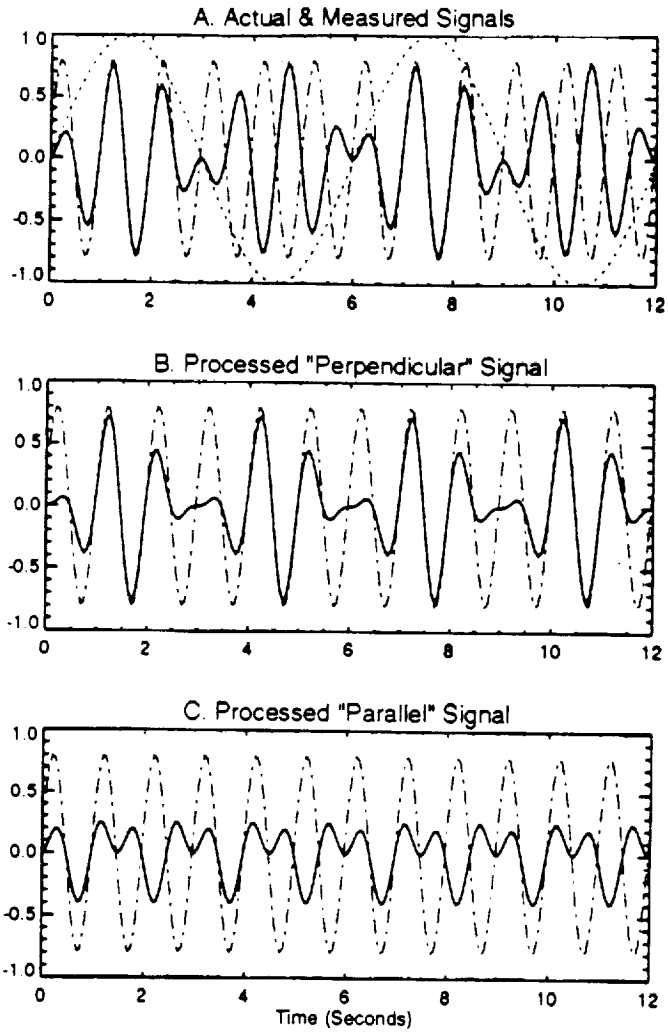
A. Actual & Measured Signals
1.0
0.5
0.0
-0.5
-1.0
0
2
4
6
8
10
12
B. Processed "Perpendicular" Signal
1.0
0.5
0.0
-0.5
-1.0
0
2
4
6
8
10
12
C. Processed "Parallel" Signal
1.0
0.5
0.0
-0.5
-1.0
0
2
4
6
8
10
12
Time (Seconds)

Figure 2

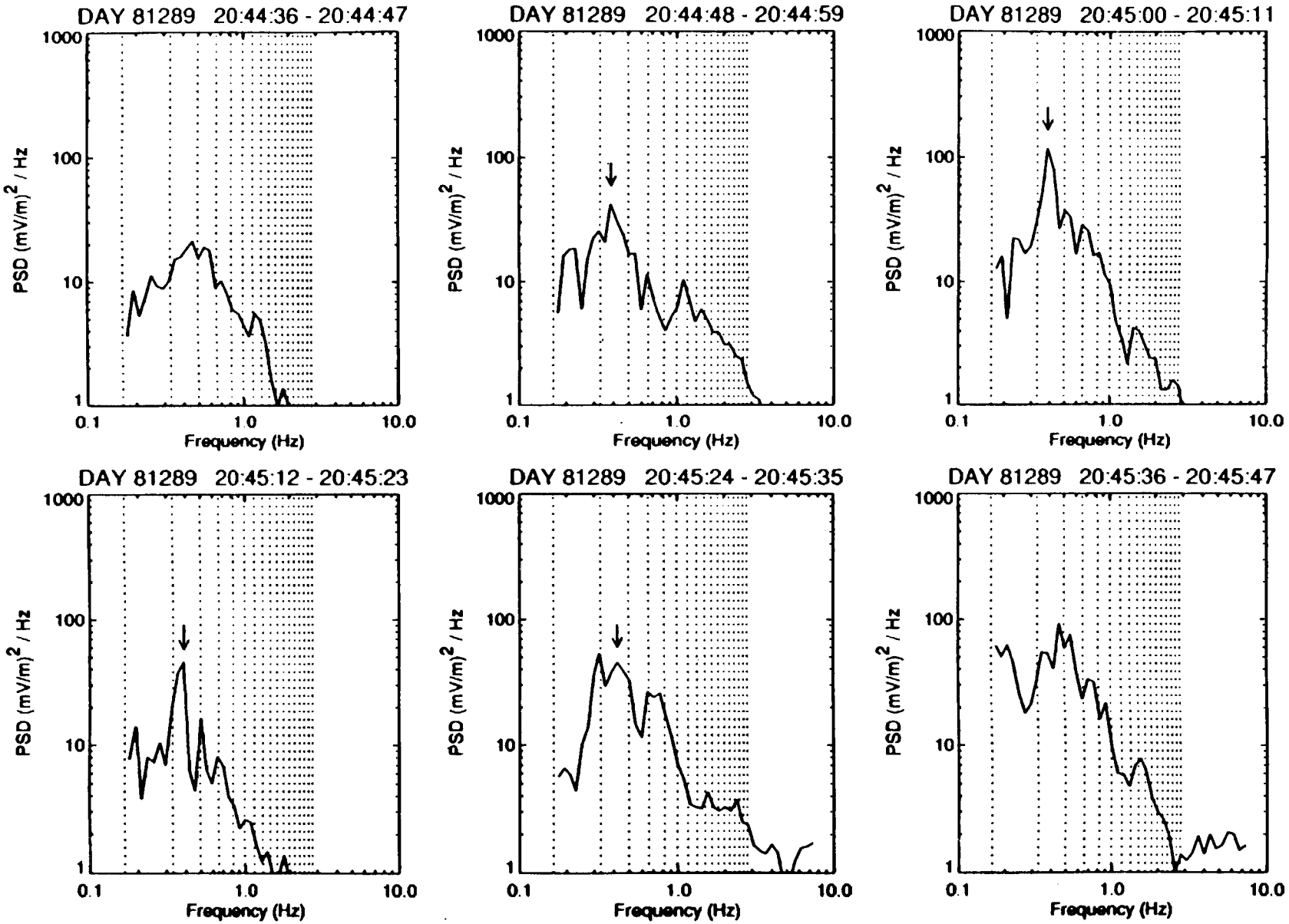
DAY 81289 20:44:36 - 20:44:47
DAY 81289 20:44:48 - 20:44:59
DAY 81289 20:45:00 - 20:45:11
DAY 81289 20:45:12 - 20:45:23
DAY 81289 20:45:24 - 20:45:35
DAY 81289 20:45:36 - 20:45:47
PSD (mV/m)^2 / Hz
Frequency (Hz)
1000
100
10
1
0.1
1.0
10.0

Figure 3

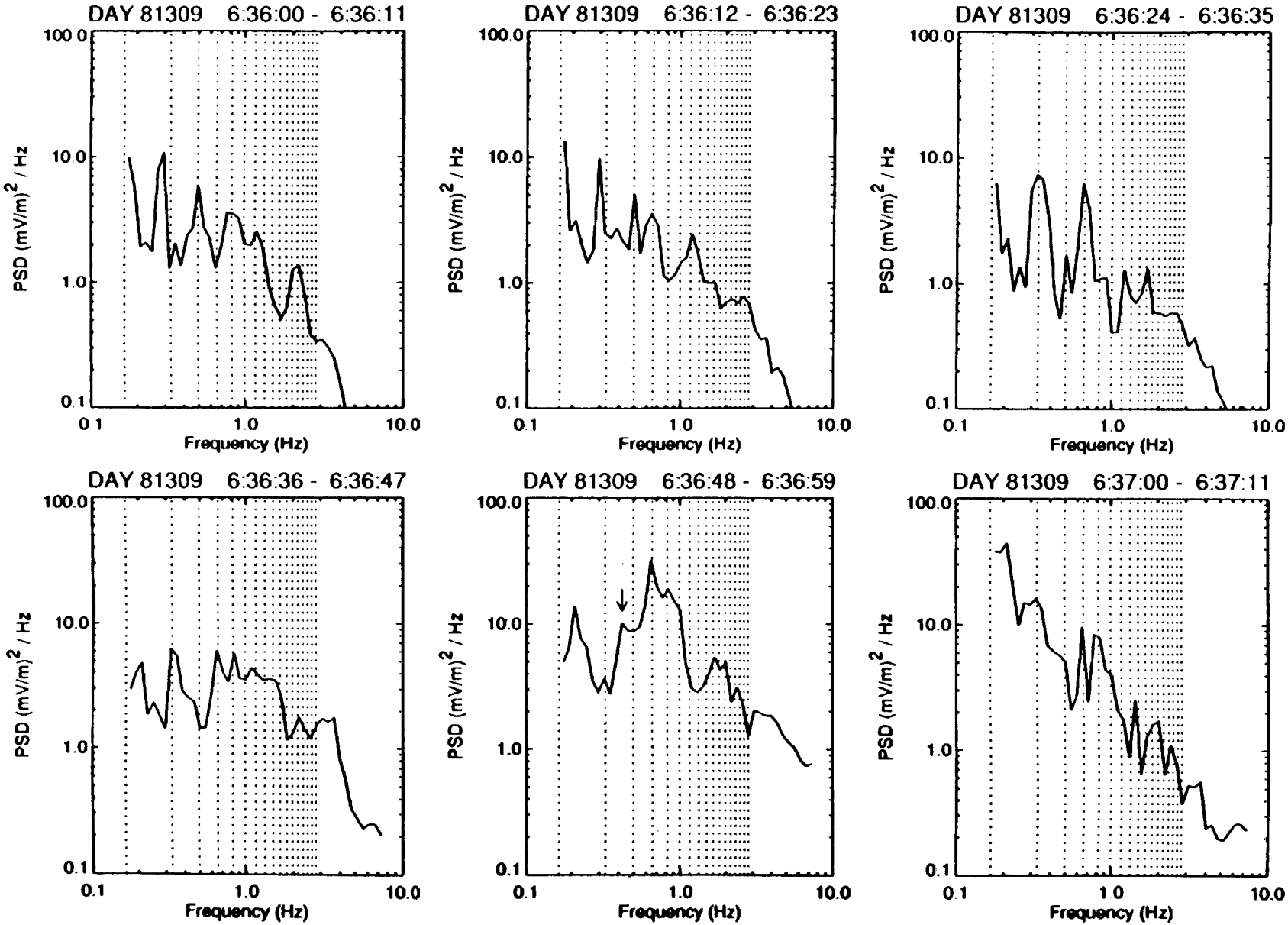
DAY 81309 6:36:00 - 6:36:11
DAY 81309 6:36:12 - 6:36:23
DAY 81309 6:36:24 - 6:36:35
DAY 81309 6:36:36 - 6:36:47
DAY 81309 6:36:48 - 6:36:59
DAY 81309 6:37:00 - 6:37:11
PSD (mV/m)^2 / Hz
Frequency (Hz)
100.0
10.0
1.0
0.1
0.1
1.0
10.0

Figure 4

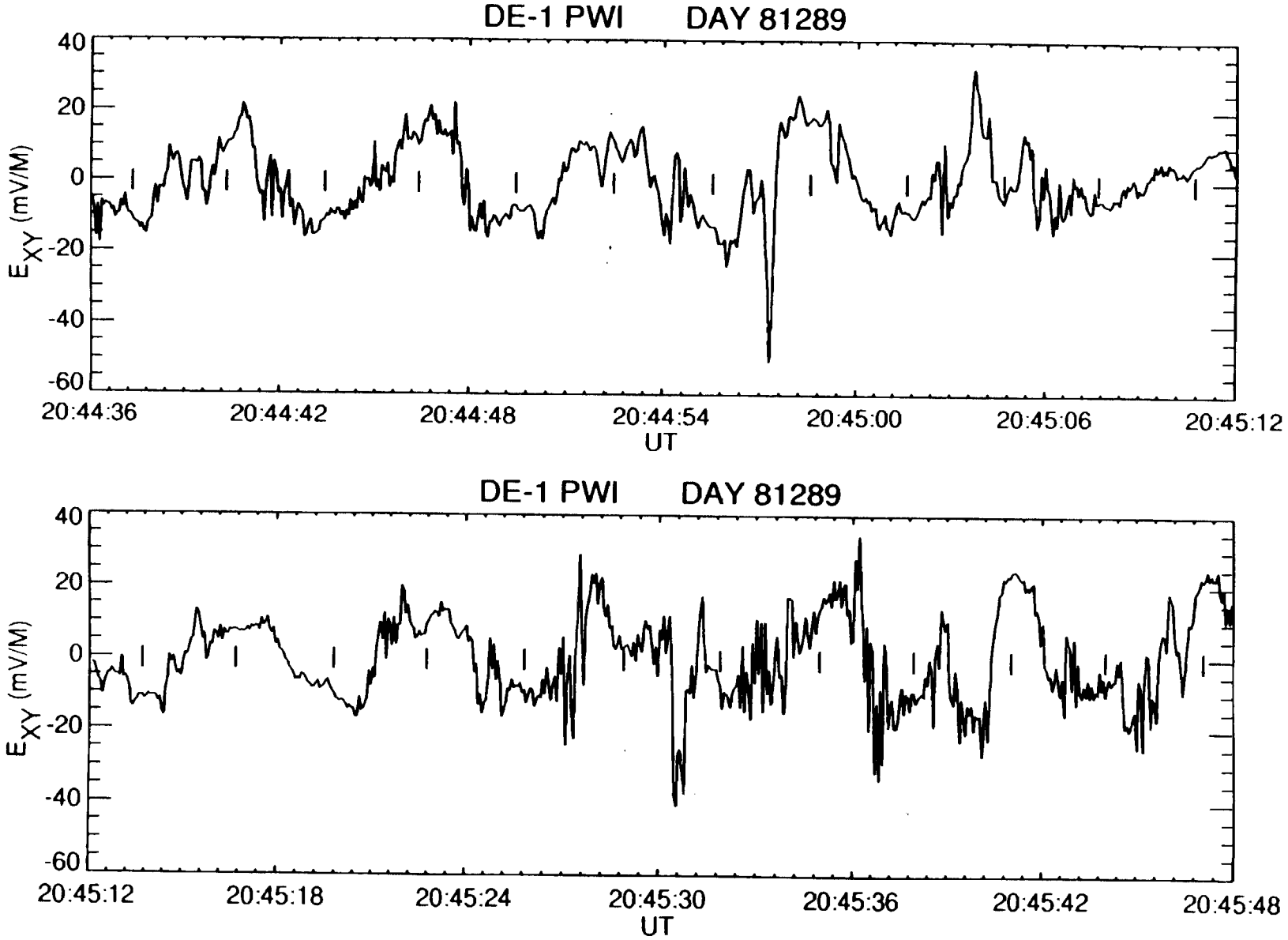
DE-1 PWI DAY 81289
40
20
0
-20
-40
-60
E_{XY} (mV/M)
20:44:36
20:44:42
20:44:48
20:44:54
20:45:00
20:45:06
20:45:12
UT
DE-1 PWI DAY 81289
40
20
0
-20
-40
-60
E_{XY} (mV/M)
20:45:12
20:45:18
20:45:24
20:45:30
20:45:36
20:45:42
20:45:48
UT

Figure 5a

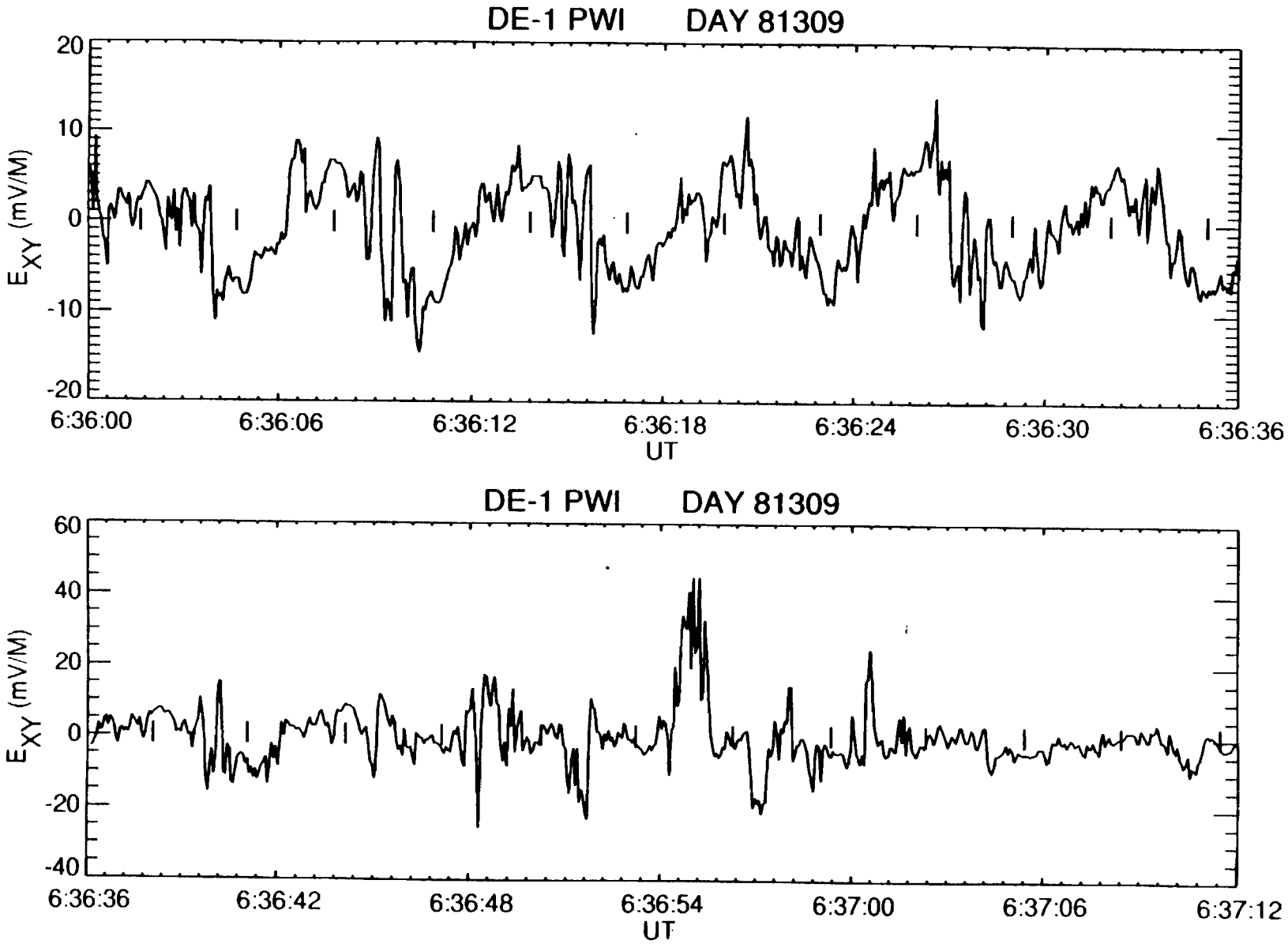
DE-1 PWI DAY 81309
20
10
0
-10
-20
E_{XY} (mV/M)
6:36:00
6:36:06
6:36:12
6:36:18
6:36:24
6:36:30
6:36:36
UT
DE-1 PWI DAY 81309
60
40
20
0
-20
-40
E_{XY} (mV/M)
6:36:36
6:36:42
6:36:48
6:36:54
6:37:00
6:37:06
6:37:12
UT

Figure 5b

A-G93-355

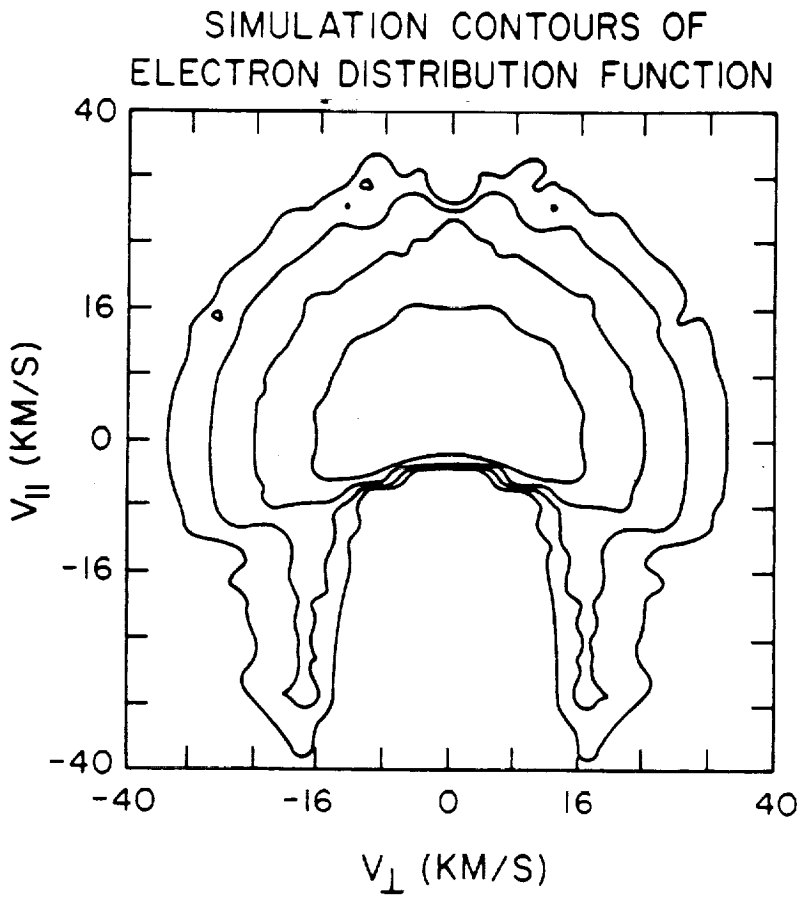

Figure 6a

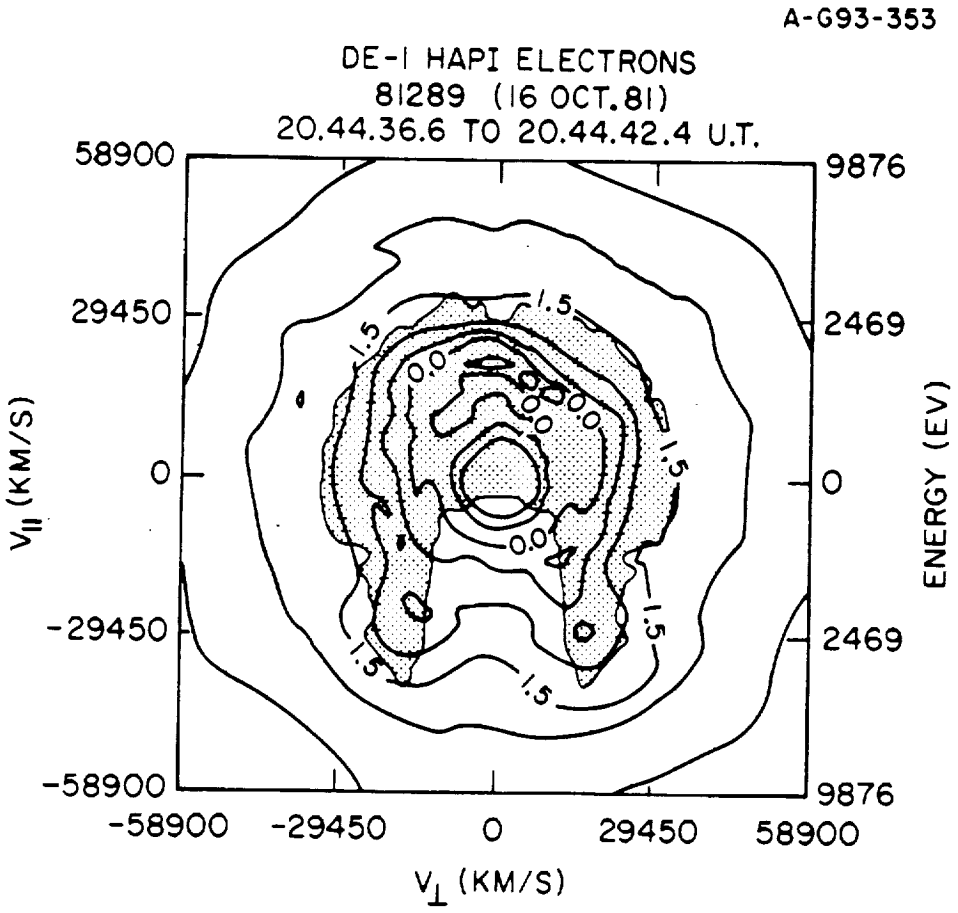
A-G93-353
DE-1 HAPI ELECTRONS
81289 (16 OCT. 81)
20.44.36.6 TO 20.44.42.4 U.T.
58900
29450
0
-29450
-58900
9876
2469
0
2469
9876
1.5
0.0
$V_{||}$ (KM/S)
ENERGY (EV)
-58900
-29450
0
29450
58900
$V_{\perp}$ (KM/S)

Figure 6b

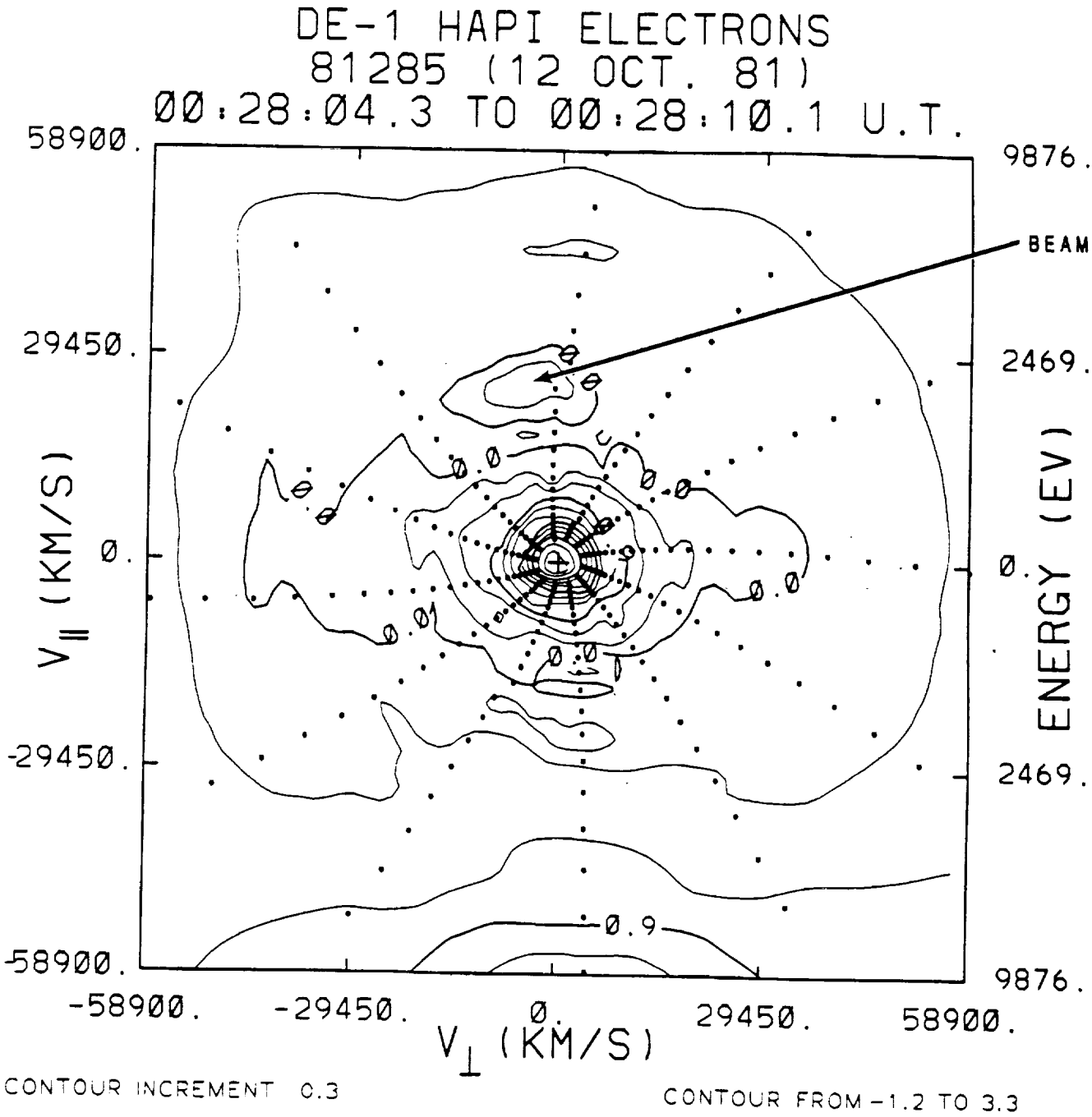
DE-1 HAPI ELECTRONS
81285 (12 OCT. 81)
00:28:04.3 TO 00:28:10.1 U.T.
58900.
29450.
0.
-29450.
-58900.
9876.
2469.
0.
2469.
9876.
BEAM
ENERGY (EV)
$V_{\parallel}$ (KM/S)
$V_{\perp}$ (KM/S)
-58900.
-29450.
0.
29450.
58900.
0.9
CONTOUR INCREMENT 0.3
CONTOUR FROM -1.2 TO 3.3

Figure 7

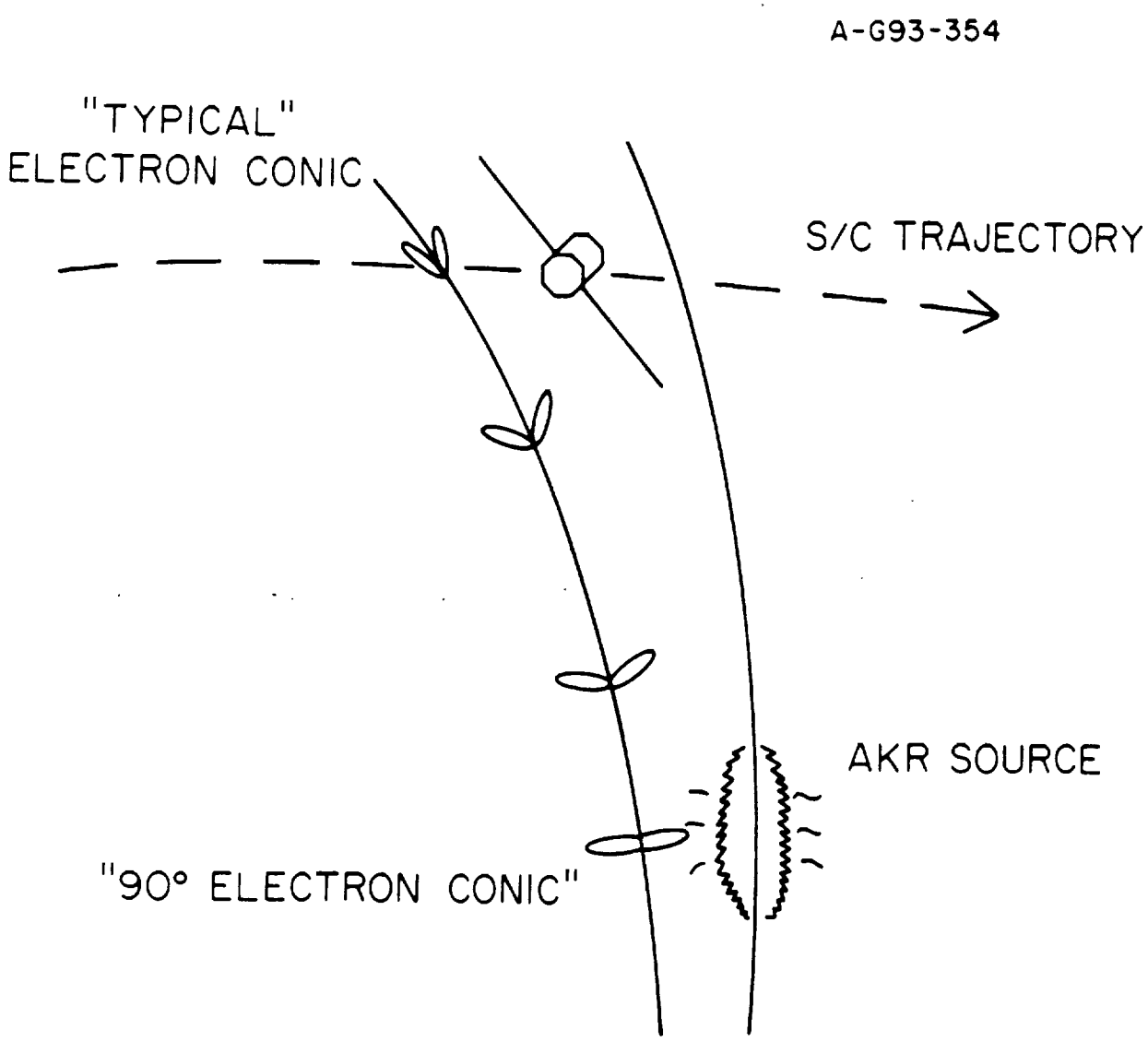
A-G93-354
"TYPICAL"
ELECTRON CONIC
S/C TRAJECTORY
AKR SOURCE
"90° ELECTRON CONIC"

Figure 8

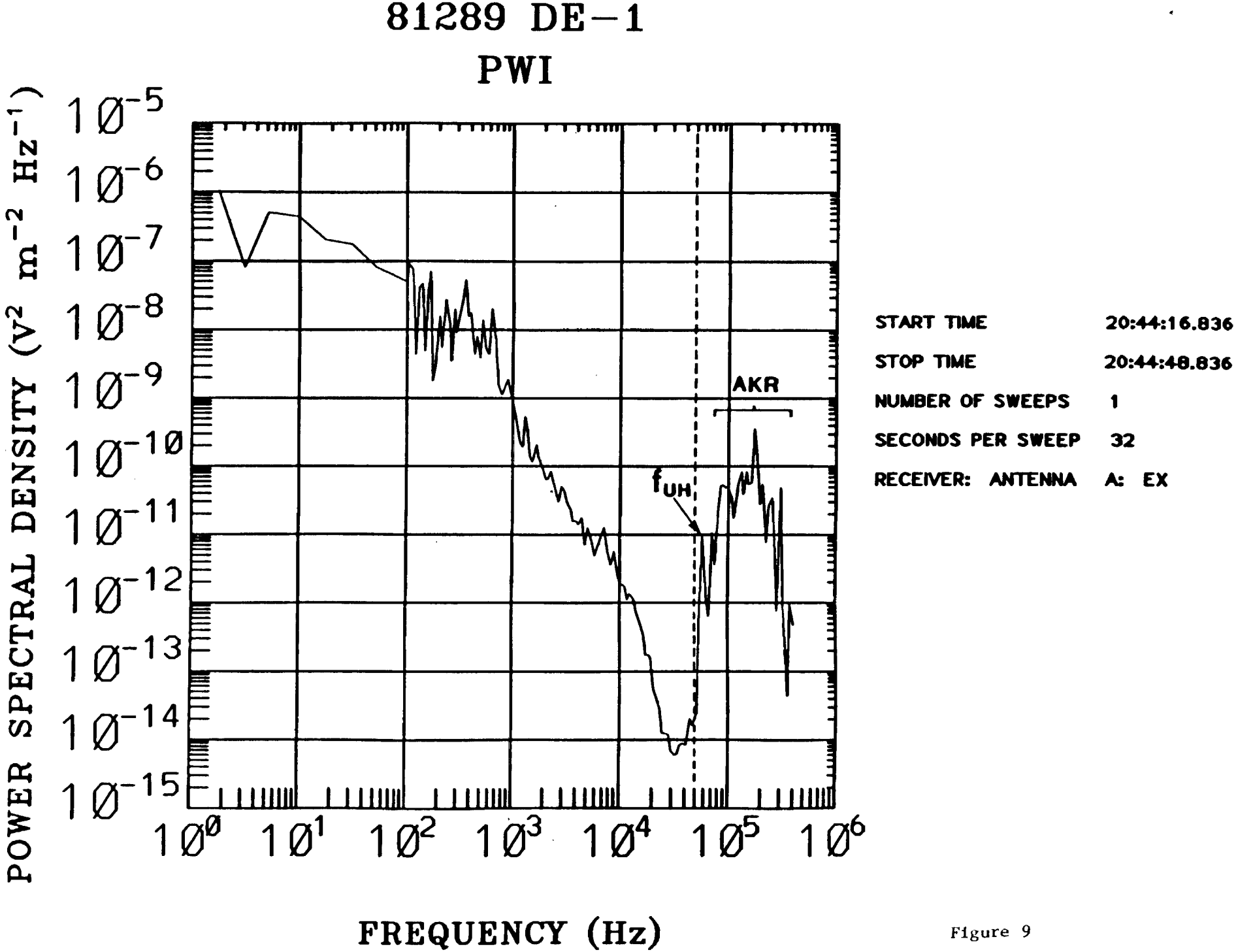
81289 DE-1
PWI
POWER SPECTRAL DENSITY (V^2 m^{-2} Hz^{-1})
10^{-5}
10^{-6}
10^{-7}
10^{-8}
10^{-9}
10^{-10}
10^{-11}
10^{-12}
10^{-13}
10^{-14}
10^{-15}
10^0 10^1 10^2 10^3 10^4 10^5 10^6
FREQUENCY (Hz)
AKR
f_{UH}
START TIME 20:44:16.836
STOP TIME 20:44:48.836
NUMBER OF SWEEPS 1
SECONDS PER SWEEP 32
RECEIVER: ANTENNA A: EX

Figure 9

waves which could contribute to oblique heating of the electrons. The dotted line indicates the location of the electron gyrofrequency.

Appendix 1

Perpendicular Electron Heating by Absorption of Auroral Kilometric Radiation

by

D. D. Morgan, J. D. Menietti, R. M. Winglee, and H. K. Wong

Abstract

We investigate the possibility of perpendicular heating of electrons and the generation of "90° electron conics" by particle diffusion in velocity space due to wave-particle interaction with intense auroral kilometric radiation. This interaction is made possible by the downward shift of the R-X cutoff below the electron cyclotron frequency that occurs in the presence of warm plasma. We simulate this condition and solve the diffusion equation using a finite difference algorithm. The results show strong perpendicular electron heating and indicate that the main characteristics of an electron conic distribution are easily reproduced under these conditions.